PHOTOSYNTHETICA 46 (3): 441-451, 2008

Conventional and combinatorial chlorophyll fluorescence imaging of tobamovirus-infected plants

M. PINEDA[*], J. SOUKUPOVÁ[**,***], K. MATOUŠ[**,***], L.NEDBAL[**,***], and M. BARÓN[*,+]

Department of Biochemistry, Molecular and Cell Biology of Plants, Estación Experimental del Zaidín, Consejo Superior de Investigaciones Científicas (CSIC), C/Profesor Albareda, nº 1, C.P. 18008, Granada, Spain[*]
Institute of Systems Biology and Ecology, Academy of Sciences of the Czech Republic, Zámek 136, Nové Hrady 37333, Czech Republic[**]
Institute of Physical Biology, University of South Bohemia, Zámek 136, Nové Hrady 37333, Czech Republic[***]

Abstract

We compared by chlorophyll (Chl) fluorescence imaging the effects of two strains of the same virus (Italian and Spanish strains of the *Pepper mild mottle virus* − PMMoV-I and -S, respectively) in the host plant *Nicotiana benthamiana.* The infection was visualized either using conventional Chl fluorescence parameters or by an advanced statistical approach, yielding a combinatorial set of images that enhances the contrast between control and PMMoV-infected plants in the early infection steps. Among the conventional Chl fluorescence parameters, the non-photochemical quenching parameter NPQ was found to be an effective PMMoV infection reporter in asymptomatic leaves of *N. benthamiana,* detecting an intermediate infection phase. The combinatorial imaging revealed the infection earlier than any of the standard Chl fluorescence parameters, detecting the PMMoV-S infection as soon as 4 d post-inoculation (dpi), and PMMoV-I infection at 6 dpi; the delay correlates with the lower virulence of the last viral strain.

Additional key words: biotic stress; *Nicotiana benthamiana*; non-photochemical quenching; *Pepper mild mottle virus*.

Introduction

Chlorophyll fluorescence imaging (Chl-FI) is a useful tool to study the spatial and temporal heterogeneity of leaf photosynthesis under biotic stress (Nedbal and Whitmarsh 2004), allowing the diagnosis and quantification of different stress responses. Changes in chlorophyll-fluorescence (Chl-F) yield could be related with physiological alterations in plants infected with bacteria (Berger *et al.* 2004, 2007, Bonfig *et al.* 2006), fungi (Scholes and Rolfe 1996, Chou *et al.* 2000, Swarbrick *et al.* 2006), and virus (Balachandran and Osmond 1994, Balachandran *et al.* 1997, Osmond *et al.* 1998, Lohaus *et al.* 2000, Chaerle *et al.* 2004). In addition, this technique was successful to monitor the effect of herbivory damage (Zangerl *et al.* 2002, Aldea *et al.* 2006, Tang *et al.* 2006).

Received 16 October 2007, *accepted* 2 May 2008.
[+]Corresponding author; fax: +34 958 12 96 00, e-mail: mbaron@eez.csic.es
Abbreviations: AS − asymptomatic; CCD − charge-coupled device; Chl − chlorophyll; Chl-F − chlorophyll fluorescence; Chl-FI − chlorophyll fluorescence imaging; dpi − days post-inoculation; F_0 − minimum chlorophyll fluorescence in the dark adapted state; F_M − maximum chlorophyll fluorescence in the dark adapted state; F_M' − maximum chlorophyll fluorescence in the light adapted state; F_M'' − maximum chlorophyll fluorescence after switching off the "actinic light" (protocol 2); F_P − maximum chlorophyll fluorescence reached at the induction curve without saturating flashes; F_t − chlorophyll fluorescence value prior to the saturating pulse in the light-adapted state; F_V − variable fluorescence; HI − high irradiance; LDA − Linear Discriminant Analysis; LED − light-emitting diode; LI − low irradiance; PAR − photosynthetically active radiation; NPQ − non-photochemical quenching; NPQ_t − non-photochemical quenching at referred kinetics times, t; P_N − net photosynthetic rate; PMMoV-I and -S − Italian and Spanish strains of the *Pepper mild mottle virus*; PS − photosystem; R − image resulting from the combinatorial imaging; Re − recovered; S − symptomatic; SFFS − Sequential Forward Floating Search; Φ_{PS2} − photosystem 2 quantum yield; $\Phi_{PS2\text{-}t}$ − photosystem 2 quantum yield at referred kinetics times, t [s].
Acknowledgements: This research and MP´s contract were supported by grants from the Spanish Ministry of Science and Education (MEC-FEDER − grant BIO2004-04968-C02-02 to MB). The cooperation between the Spanish and the Czech groups was carried out in the frame of the Exchange Programme CSIC/Academy of Sciences of the Czech Republic (projects 2003CZ0011 and 2004CZ0016). JS was supported by the Czech Ministry of Education, Sports, and Youth (grant MSM6007665808) and the Academy of Sciences of the Czech Republic (grant AVOZ60870520). The authors thank Drs. I. García-Luqje and M. Serra for the gift of PMMoV-solutions.

Modern Chl-FI instruments support complex measuring protocols with different darkness-adaptation times of the plant, combined with periods of constant "actinic light", both supplemented by saturating bright flashes. In practice, various types of irradiance protocols have been used to reveal differences between healthy and stressed plants: determining Chl-F values after just one saturating flash (Chaerle *et al.* 2004, 2006), Kautsky kinetics (Kautsky and Hirsch 1931; reviewed in Lichtenthaler and Babani 2004), harmonic oscillations (Nedbal and Březina 2002, Nedbal *et al.* 2003, Matouš *et al.* 2006), quenching analysis with different numbers of saturating flashes (Pérez-Bueno *et al.* 2006), and combined with various "actinic light" irradiances (Matouš *et al.* 2006, Berger *et al.* 2007).

In fluorescence induction experiments and quenching analysis, copious information is obtained with a great number of Chl-F parameters associated with the photosynthetic function; the calculation of these parameters is based on the pulse-amplitude technique established by Schreiber *et al.* (1986). Some coefficients are related to photochemical processes: F_V/F_M (Kitajima and Butler 1975) and Φ_{PS2} represent the maximum and effective quantum yields of photosystem 2 (PS2) (Genty *et al.* 1989); the non-photochemical processes are typically represented by NPQ (non-photochemical quenching; Bilger and Björkman 1990). The R_{FD} coefficient related to plant vitality (Lichtenthaler and Rinderle 1988) has also been broadly used. Lists of many other Chl-F parameters related to different physiological functions have been reviewed (*e.g.* Schreiber *et al.* 1986, Roháček and Barták 1999, Maxwell and Johnson 2000). Images of such conventional Chl-F parameters could provide a good early stress indicator to follow pathogenesis (Pérez-Bueno *et al.* 2006).

However, standard Chl-F parameters do not always reach a sufficient contrast between healthy and infected tissues. In this context, Soukupová *et al.* (2003) proposed a simple algorithm to quantify the capacity of the individual Chl-F parameters in detecting effects of fungal phytotoxins in *Brassica napus* and white mustard. More recently, Matouš *et al.* (2006) and Berger *et al.* (2007) described a combinatorial imaging method to map bacterial infection in *Arabidopsis*. This method searches for small sets of images, obtained during Chl-F transient, that offer the highest contrast between the stressed and control leaf tissue and that can be effectively used to visualize the pathogenic action during the early infection phase.

Here, the experimental host-pathogen system studied was *Nicotiana benthamiana* plants infected with the Italian and Spanish strains of the *Pepper mild mottle tobamovirus* (PMMoV-I and -S, respectively). They were isolated in Sicily (Italy) and Almería (Spain), respectively (Wetter *et al.* 1984, Alonso *et al.* 1989). PMMoV-I is less virulent than PMMoV-S (García-Luque *et al.* 1993, Rahoutei *et al.* 2000) and only PMMoV-I-infected plants could recover from their symptoms (Chaerle *et al.* 2006). Infection with both tobamoviruses causes serious economic losses worldwide in pepper crops (Alonso *et al.* 1989, Lamb *et al.* 2001).

In previous studies (Barón *et al.* 1995, Rahoutei *et al.* 1998, 1999, 2000, Pérez-Bueno *et al.* 2004) we have proposed the oxygen-evolving complex as the primary target of these tobamoviruses on the electron transport chain. Chl-FI studies of *N. benthamiana* plants infected with PMMoV-I revealed that NPQ was a good reporter of the infection process in leaves which remain asymptomatic (AS) during the infection process, paralleling the spread of the virus in these leaves (Pérez-Bueno *et al.* 2006). Chaerle *et al.* (2006) detected thermal and Chl-F responses in *N. benthamiana* plants infected with either PMMoV-I or -S. They found that PMMoV-S induced earlier alterations than PMMoV-I in the Chl-FI pattern of AS leaves from infected plants, in accordance with the different virulence of the viral strains. However, the first reporter of viral infection was the temperature increment registered near the main veins.

The aim of the present study was to further investigate possibilities of an early detection of the infection of *N. benthamiana* plants by the above mentioned two strains of the same virus. In addition, we tried to identify the differences between the infection progresses induced by these two tobamoviruses. We used imaging of conventional Chl-F parameters as well as combinatorial imaging (Matouš *et al.* 2006, Berger *et al.* 2007). These techniques were primarily compared in their capacity to resolve the early infection phases.

Materials and methods

Plant and virus: *N. benthamiana* Gray plants were cultivated in a growth chamber at 100 μmol(photon) m^{-2} s^{-1} PAR (photosynthetically active radiation), generated by cool white fluorescent lamps, with a 16/8 h light/dark photoperiod, a temperature regime of 24/18 ºC (day/night), and a relative humidity of 65 %.

At the 6−7 fully-expanded-leaf stage, plants were mechanically-inoculated with PMMoV in the three lower leaves, using carborundum powder and 25 μm^3 of inoculum per leaf (50 μg of tobamovirus per cm^3 of 20 mM sodium phosphate/bisphosphate buffer, pH 7.0). Two strains of PMMoV were used in the experiment: Italian (PMMoV-I) and Spanish strain (PMMoV-S). Control mock-inoculated plants were treated with buffer only. All the results of this work have been obtained comparing control mock plants with infected ones. Starting with the lowest inoculated leaf and numbering leaves in ascending order, we have analysed leaf number 5 as the AS one.

Chl fluorescence measurements were performed by a commercial kinetic Chl fluorescence instrument (*FluorCam*, *Photon System Instruments PSI*, Brno, Czech Republic; www.psi.cz), described by Nedbal *et al.* (2000). Chl-F emission from a leaf was excited by two panels of light-emitting diodes (LEDs) ($\lambda_{max} \approx 635$ nm) that generate measuring flashes (10 μs) and "actinic light". Brief and intense saturating radiation pulses [1 500 μmol(photon) m^{-2} s^{-1}, 1 s] were generated by a 250-W "white" (λ = 400−700 nm) halogen lamp. The Chl-F emission transients are captured by a CCD (charged coupled device) camera in series of images at 12-bit resolution in 512×512 pixels, taking fifty images per second. The reflected radiation is blocked by a far-red filter (*RG697*, *Schott*, Mainz, Germany).

All measurements were carried out in attached leaves. The Chl-F transients of AS leaves were elicited by three measuring protocols (Fig. 1):

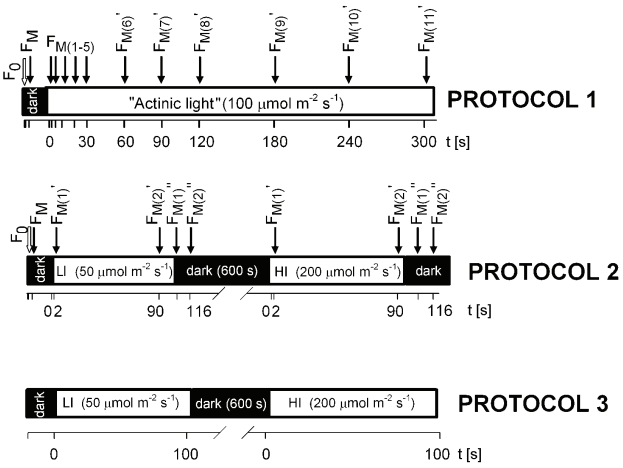

Fig. 1. Schematic description of the three protocols used in this work for measuring attached AS leaves. *Dark boxes* show the dark periods in every measurement. The irradiance by "actinic light" applied in every protocol is indicated in *the white boxes*. The *white arrows* display the moment of F_0 measurement. Every *black arrow* shows the saturating flashes applied to the AS leaves [1 500 μmol(photon) m^{-2} s^{-1}]. Over every black arrow a legend indicates if the obtained Chl-F value corresponds to F_M, F_M', or F_M''.

Protocol 1: This quenching analysis was previously described by Pérez-Bueno *et al.* (2006). Here, F_0 and F_M measurements on dark-adapted leaves were followed by 16 s of dark (Fig. 1, *upper row*). Then, the leaves were irradiated with continuous "actinic light" corresponding to the cultivation irradiance [100 μmol (photon) m^{-2} s^{-1}] for 302 s, supplemented with 11 saturating pulses to measure F_M' [at 2, 5, 10, 20, 30, 60, 90, 120, 180, 240, and 300 s of "actinic light"]. Four repetitions of the infection process were done, with four plants for every treatment (control, PMMoV-I and PMMoV-S infected).

Protocol 2: This quenching analysis was carried out using two "actinic light" irradiances and four saturating radiation pulses (Fig. 1, *middle row*). After measurements of F_0 and F_M, a short dark relaxation (16 s) followed. Then, the leaf was exposed to a low "actinic light" [LI, 50 μmol(photon) m^{-2} s^{-1}] for 100 s and the corresponding Chl-F induction was recorded. Two saturation pulses at 2 and 90 s after switching on the "actinic light" were applied to measure $F_{M(1)}$' and $F_{M(2)}$', respectively, to probe the irradiation-induced quenching. A short dark adaptation (16 s) followed by two other saturating pulses (5 s = $F_{M(1)}$'' and 16 s = $F_{M(2)}$'' after switching off the "actinic light") allowed the measurement of NPQ recovery. These measurements were followed by 600 s of dark adaptation and then by an identical sequence of measurements under higher "actinic light" irradiance [HI, 200 μmol(photon) m^{-2} s^{-1}]. The experiment was performed with twelve plants (four repetitions for control, PMMoV-I and PMMoV-S infected plants).

Using protocols 1 and 2, the following parameters were calculated according to Maxwell and Johnson (2000):

non-photochemical quenching: $NPQ = (F_M - F_M')/F_M$
effective quantum yield of PS2: $\Phi_{PS2} = (F_M' - F_t)/F_M'$

Protocol 3: After F_0 measurements on dark-adapted leaves, the Chl-F induction curve (Kautsky effect) was measured under continuous "actinic" irradiance at both LI and HI (Fig. 1, *bottom row*). A dark period (600 s) was separating LI and HI measurements. The experiment was also performed with twelve plants (four repetitions for control, PMMoV-I and PMMoV-S infected plants).

Image selection and data analysis: A large amount of information was compiled as a function of the post-infection time, virus strain, and selected Chl-F parameter. Images of the Chl-F parameters showing the highest contrast between leaves of control and infected plants were selected. NPQ and Φ_{PS2} were the best indicators of the PMMoV infection, as described in Results. Images of both standard and novel Chl-F parameters showing marked differences between control and infected leaves were displayed in false-colour scale.

Chl-F transients were obtained by integrating signal over the entire leaf area when measuring protocols 2 and 3 were applied.

Combinatorial imaging: The technique of combinatorial imaging is described in detail in Matouš *et al.* (2006) and Berger *et al.* (2007). This method was applied on data obtained by the most complex protocol 2. Here, we trained the algorithm using data of plants infected with PMMoV-S at 16 d post-inoculation (dpi), because of the higher virulence of this viral strain (García-Luque *et al.* 1993, Rahoutei *et al.* 2000). Moreover, at 16 dpi the symptoms were relatively strong; thus, the assessment of classification performance was possible. In this "training"

process, we found sets of three Chl-F images that yielded maximum contrast between control (4 plants) and PMMoV-S infected plants (4 plants) (classification performance) at 16 dpi using Sequential Forward Floating Search algorithm (SFFS, Pudil *et al.* 1994, Matouš *et al.* 2006). Here, each set of three Chl-F images was evaluated by SFFS for its capacity to discriminate the control and infected plants. In this process, any arbitrarily selected pixel in the testing Chl-F image was compared to homologous training sets of control and infected plant images. If its Chl-F levels were more similar to the infected plants, the pixel was classified as "infected", otherwise it was classified as "healthy". Then, we used the *a priori* knowledge as to what plant this particular pixel belonged to and decided if the classification was correct or erroneous. The subset of Chl-F images that yielded the lowest error rate and, thus, the highest performance was selected as the most contrasting images for combinatorial imaging in the system PMMoV-*N. benthamiana.* The classification was carried out by Linear Discriminant Classifier (Fukunaga 1990).

After identification of the set of the three most contrasting images (features), the LDA (Linear Discriminant Analysis) algorithm (Fukunaga 1990) was used to find their linear combination into one-dimensional artificial parameter R. Once the R parameter was calculated, its distribution in all measured leaves (controls, PMMoV-I and PMMoV-S infected) at different dpi was further used to follow the viral infection. The resulting image (the distribution of R in leaves) was shown in false colour scale. The resulting images express similarity of the pixels of the measured leaf, at the particular dpi, to the training sets of healthy or infected plants, respectively.

In this study, the R distribution was used to evaluate the difference between control and infected plants; and thus to reveal the infection symptoms at its early stage. The R parameter has no physiological meaning and it is specific for this particular infection in the above-mentioned cultivation conditions.

Results

Visual symptoms: First symptoms, consisting in the appearance of new curly young leaves, were visible in PMMoV-infected plants from 5−7 dpi onwards (PMMoV-S and -I, respectively; Fig. 2*A,B*). We have focused this study in the AS leaves, that were totally developed at the time of infection and did not show any symptoms during the infection process (Fig. 2*A,C*). Growth was inhibited in plants infected with either one of the virus strains, being evident at 14 dpi (Fig. 2*A*). At 24 dpi, plants infected with PMMoV-S were totally senescent, and were no longer measured; whereas PMMoV-I-infected plants started to recover from the symptoms (as evaluated by emergence of new unaffected leaves and an internode elongation) from 21−28 dpi (Fig. 2*D,E*).

Study of standard Chl-F parameters during quenching analysis (protocol 1): We have analyzed various conventional Chl-F parameters in order to find those that can discriminate the two infections with two similar strains of the PMMoV in the early infection stages and in the absence of symptoms. By empiric qualitative inspection, we found that NPQ and Φ_{PS2} were the highly effective Chl-F parameters detecting PMMoV infection in *N. benthamiana* plants (Fig. 3), in contrast to other conventional parameters as F_V/F_M, R_{FD}, q_{TQ} (total quenching; Roháček and Barták 1999), or q_{CN} (complete non-photochemical quenching; Roháček and Barták 1999) (data not shown).

The earliest changes on NPQ pattern discriminating infected and control plants were detected at 17 dpi, as shown in Fig. 3*A*. Saturating irradiance that elicited hardly any NPQ in control plants (*top row*), led to a high and sustained NPQ in AS leaves of PMMoV-I infected plants (*middle row*). The NPQ in PMMoV-S plant (*bottom row*) was stronger than in controls (*top row*) but somewhat weaker than in PMMoV-I plant (*middle row*). A heterogeneous pattern of NPQ in the AS leaves of infected plants was observed, consisting of different NPQ values in leaf tissue surrounding the main veins and in the intervein tissue. The NPQ pattern started to be visible in NPQ images taken 20 s after switching on the "actinic light" (NPQ_{20}); the highest overall contrast was achieved at 60 s and persisted up to 240 s.

Fig. 3*B* displays the dynamics of NPQ_{20} distribution over the leaves during the first 28 dpi. NPQ_{20} (NPQ measured after 20 s of the "actinic light" exposure) was the kinetic point showing the greatest differences between control and PMMoV-infected plants over the entire infection period. Prior to 17 dpi, we could not find any significant response in NPQ_{20} pattern. Starting at 17 dpi, AS leaves of the infected plants developed characteristic NPQ_{20} patterns. Considering the signal over the whole leaf, NPQ was higher in the infected plants compared to control at 17 dpi (Fig. 3*A*) and the relationship became inverse between 19 and 28 dpi (Fig. 3*B*). At 24 dpi, plants infected with PMMoV-S were already senescent, and were no longer measured.

The analysis of the spatial pattern of Φ_{PS2}, another frequently used Chl-F parameter, displayed differences between PMMoV-S infected and control plants, first at 17 dpi. A specific Φ_{PS2} pattern in infected plants was only evident at 2 s after switching on the "actinic light" ($\Phi_{PS2\text{-}2}$) (data not shown). We have followed the progress of $\Phi_{PS2\text{-}2}$ pattern of control and infected leaves throughout the infection period (Fig. 3*C*). Between 17−24 dpi, AS leaves of PMMoV-S-infected plants displayed a characteristic spatial pattern, with higher $\Phi_{PS2\text{-}2}$ in the tissues

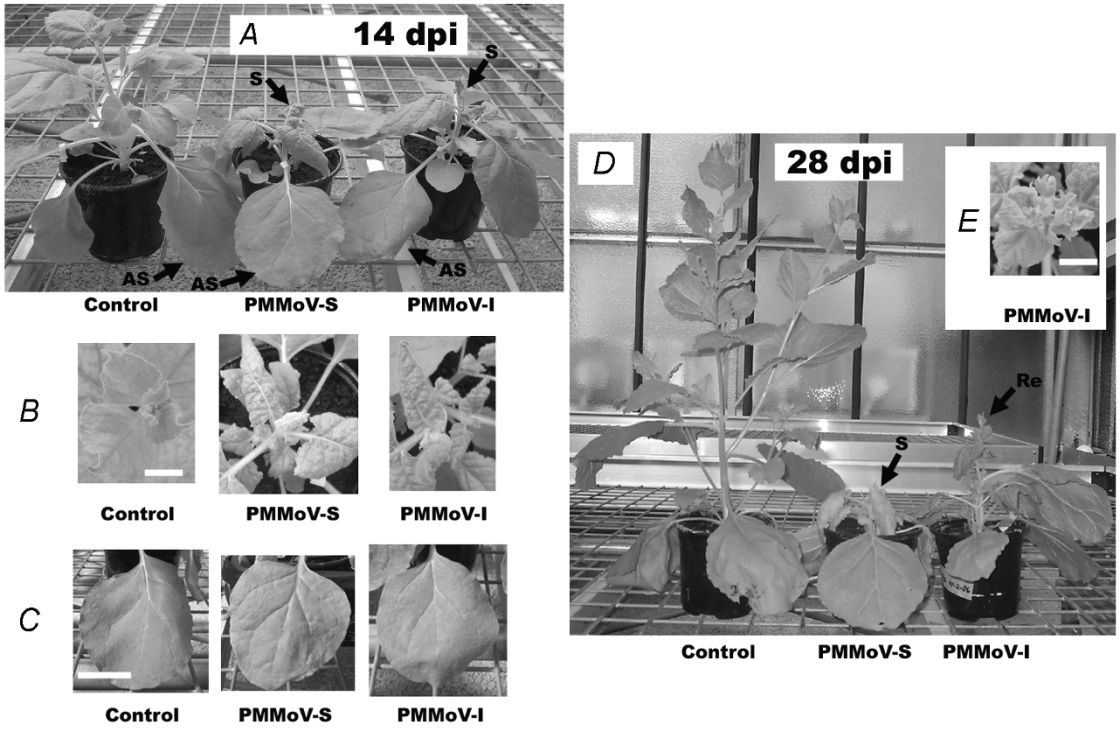

Fig. 2. Symptomatology of *Nicotiana benthamiana* plants infected with PMMoV, compared with their respective control plants. (*A*) Representative images of control, PMMoV-S- and PMMoV-I-infected plants at 14 dpi. (*B*) Detail of the S (symptomatic) curled leaves of PMMoV-infected plants and their corresponding controls at 7 dpi (*size bar*: 10 mm). (*C*) Detail of the AS (asymptomatic) leaves of PMMoV-infected plants and the corresponding control leaves at 17 dpi (*size bar*: 40 mm). (*D*) Images of control and infected plants at 24 dpi, displaying the symptom recovery phase in PMMoV-I-infected plants. Re − recovered leaves. (*E*) Detail of a PMMoV-I infected plant at 28 dpi, showing the emergence of new unaffected leaves (*size bar*: 10 mm).

surrounding the main veins than in intervein tissues. The $\Phi_{PS2\text{-}2}$ pattern was more homogeneous throughout the whole leaf in case of PMMoV-I and control plants. This feature of PMMoV-S infection can be considered for differentiation from PMMoV-I.

Analysis of Chl-F parameters and Chl-F kinetics (protocol 2): Using the protocol 1, we did not detect any PMMoV-induced changes on the Chl-F parameters prior to 17 dpi. Matouš *et al.* (2006) and Berger *et al.* (2007) showed that the resolving capacity of Chl-FI depends on the measuring protocol. Thus, we have used a complex protocol with two different "actinic light" irradiances. The Chl-F kinetics of control and infected plants were compared, analysing separately the results obtained under HI and LI.

As expected, the first differences between control and PMMoV-infected plants were detected at 16 dpi in the NPQ pattern under LI (Fig. 4*A*) and HI (Fig. 4*B*): The NPQ images of the AS leaves obtained at the first saturating pulse in the dark under both LI and HI, where the difference in the NPQ pattern between control and infected leaves was the highest. Significant heterogeneity in NPQ pattern developed in NPQ at 16 dpi, whereas no changes were seen at 9 dpi. The heterogeneity was stronger under HI (Fig. 4*B*) than under LI (Fig. 4*A*). Other conventional Chl-F parameters obtained by the protocol 2 did not perform better than NPQ shown in Fig. 4.

In another attempt to find differences between the control and infected plants, we integrated the Chl-F signal over the entire leaf surface and identified differences between the F_0-normalized Chl-F transients measured by protocol 2 (Fig. 5). First differences were observed at 13 dpi under LI, becoming well pronounced at 16 dpi under both irradiances. The largest differences were seen in the Chl-F decline following the local transient maximum F_P.

Analysis of Kautsky kinetic (protocol 3): Since the strongest differences between Chl-F transients of control and infected plants were found during the Chl-F decline from F_P, we applied protocol 3, which was focused on detailed monitoring of Kautsky-type induction under LI and HI (Fig. 6*A,B*, *left panels*).

The Chl-F kinetics of PMMoV-infected plants changed with the infection progress and significant differences were found compared with the controls. Remarkable differences between Chl-F transients of control and infected plants were found in the first phase of the induction transient: during the rise to F_P and the subsequent decline (Fig. 6*A,B*, *right panels*). At 9 dpi, transients of PMMoV-infected plants differed from that of control

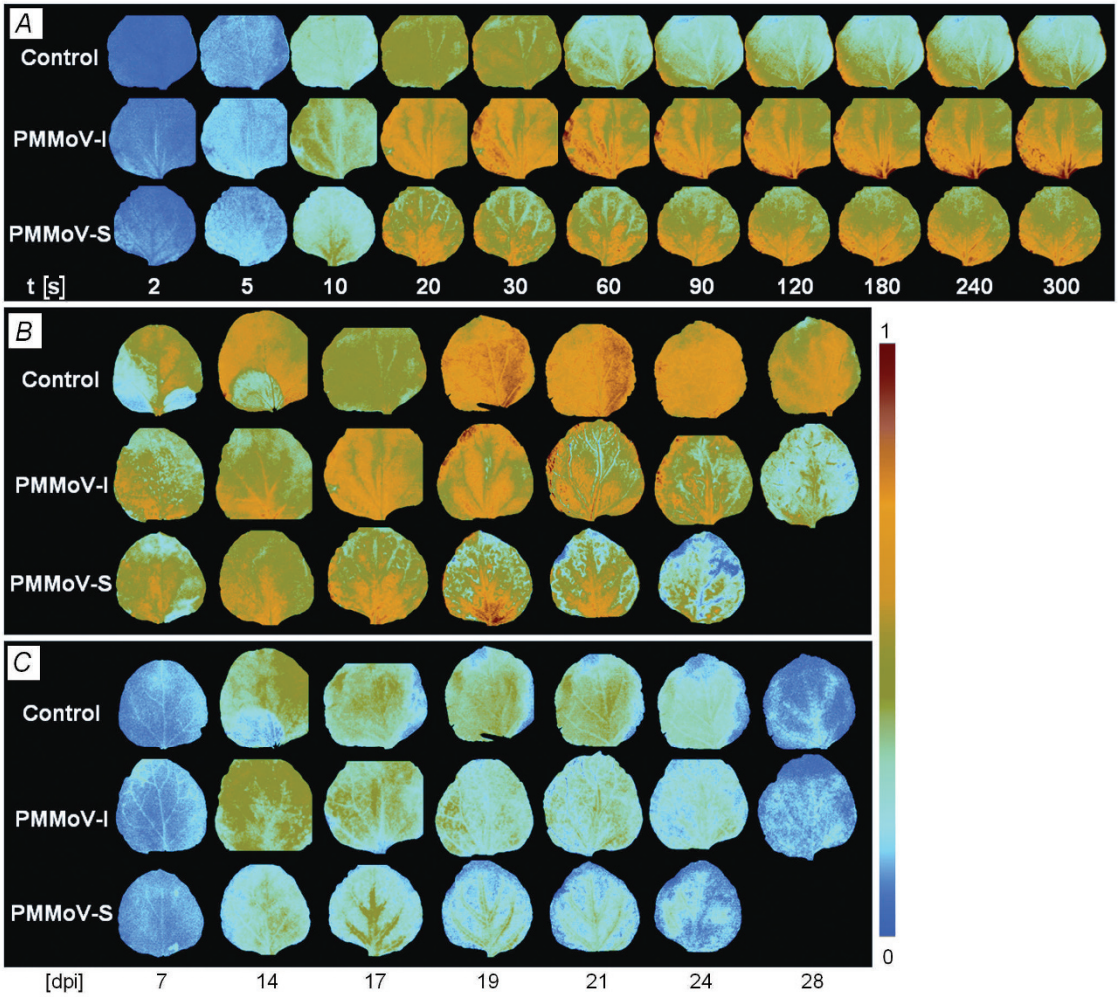

Fig. 3. Images of non-photochemical quenching (NPQ) and photosystem 2 quantum yield (Φ_{PS2}) obtained from measurements using protocol 1 in AS leaves from control and PMMoV-infected plants. Chl-F images are shown for representative samples. (*A*) Transient of NPQ during the chlorophyll fluorescence induction kinetics at 17 dpi. (*B*) NPQ_{20} (NPQ at 20 s after the onset of "actinic light") pattern at different dpi (displayed at the bottom of the figure). (*C*) $\Phi_{PS2\text{-}2}$ (Φ_{PS2} at 2 s after switching on the "actinic light") pattern at different dpi. The *colour scale* indicates the amplitude of every fluorescence parameter.

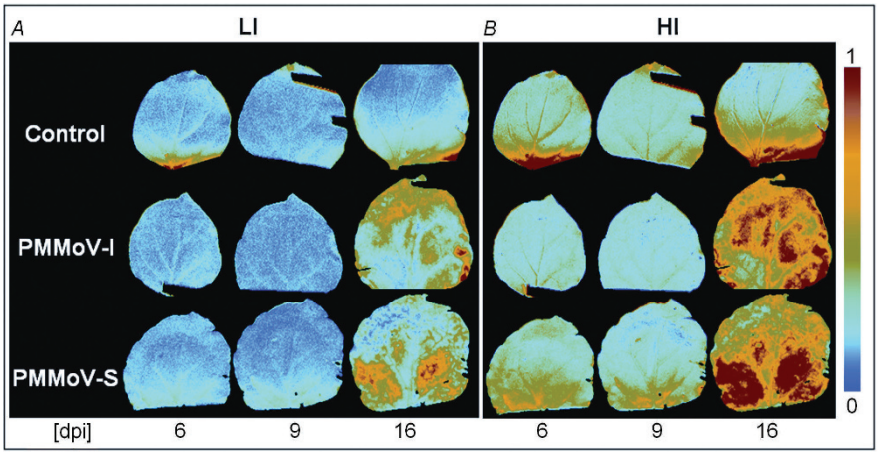

Fig. 4. NPQ images of AS leaves from measurement by protocol 2 at different dpi (indicated at the bottom) in plants exposed at low (*A*) and high (*B*) "actinic light". NPQ was measured during an early phase of quenching relaxation, 5 s after switching off the "actinic light". LI: 50 μmol(photon) m^{-2} s^{-1}; HI: 200 μmol(photon) m^{-2} s^{-1}. NPQ images are shown for representative samples.

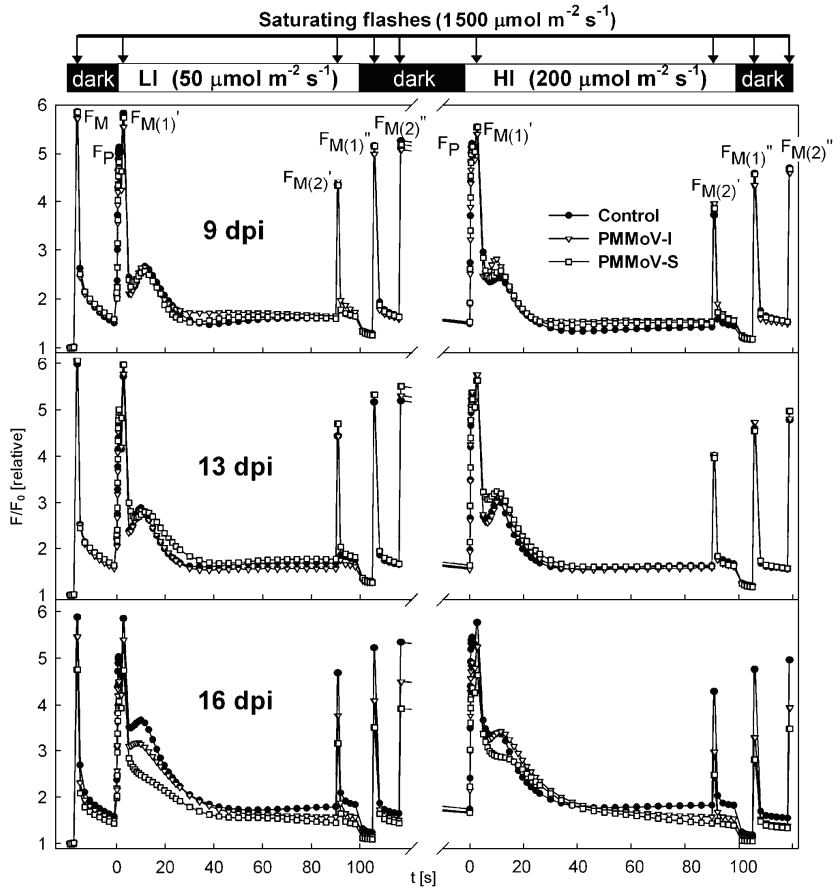

Fig. 5. Chl-F transients of AS leaves measured with protocol 2 at different dpi. A brief description of the protocol is provided at the top of the figure, and the distinct peaks (F_M, F_P, $F_{M(1)}'$, $F_{M(2)}'$, $F_{M(1)}''$, and $F_{M(2)}''$) are depicted in the 9 dpi transient Chl-F kinetic. LI: 50 μmol(photon) m^{-2} s^{-1}; HI: 200 μmol(photon) m^{-2} s^{-1}. Individual Chl-F transients represent averaged Chl-F signal over the four measured leaves (controls, PMMoV-I and PMMoV-S infected plants). Fluorescence values were normalized to F_0.

at 1 s (F_1/F_0) and 5 s (F_5/F_0) after switching on the incident irradiance. The ratio F_5/F_0 yielded a significant contrast both under LI and HI, with the difference being slightly higher in HI. Although at 13 dpi this feature persisted even at lower values, another differential feature appeared at 7 s, which was associated with the PMMoV-S infection, and the difference between the transient of PMMoV-I infected plant and control was lower (<10 %). At 16 dpi the transients from control and infected plants differed in various time points.

The empirical selection of F_5/F_0 to reveal PMMoV infection in *N. benthamiana* was confirmed by imaging this parameter during the early infection phase (Fig. 7). AS leaves of infected plants showed a spatial pattern of F_5/F_0 under HI at 9 dpi. The intensity of the Chl-F signal surrounding main veins in these leaves is lower than in the rest of the leaf blade (Fig. 7). At 13 and 16 dpi (*middle and right columns*), the AS leaves of infected plants showed a higher value for this parameter in the intervein parts, starting from the edges. Chl-F signal of control leaf remained low and homogeneous until 16 dpi. The parameter F_5/F_0 was more capable in resolving the PMMoV infection than the often used conventional parameters NPQ and Φ_{PS2}.

Combinatorial imaging (protocol 2): The contrast in the standard Chl-F parameters between infected and control leaves was sub-optimal in the experiments that we have already described. To find the maximum contrast between the control and infected leaves, we applied the combinatorial imaging method (see Materials and methods, Matouš *et al.* 2006) to the data obtained by protocol 2 that probed the entire Chl-F transient. We found as the most contrasting images [*I(t)*] those taken at times t_1 = 5 s, t_2 = 21 s, and t_3 = 736 s (*i.e.* at 5 and 21 s of LI, and 16 s of HI). These images are not important for this viral detection when they are used separately, but their combination is strong enough for this purpose. The optimal linear combination was:

$$R = -0.155\ I(5\ s) - 0.574\ I(21\ s) + 0.804\ I(736\ s)$$

R is the resultant one-dimensional artificial parameter without any physiological interpretation, expressing only the contrast between infected and healthy plants, with no units, and no meaning of the constants in the equation. Fig. 8 shows the resulting combinatorial images (R) of AS leaves from controls as well as PMMoV-I and PMMoV-S infected plants at different dpi. The resulting image R was calculated pixel-by-pixel according to above mentioned equation and shown in false colour scale. Using this approach, the PMMoV infection was detected already at 4 and 6 dpi (for PMMoV-I and -S, respectively).

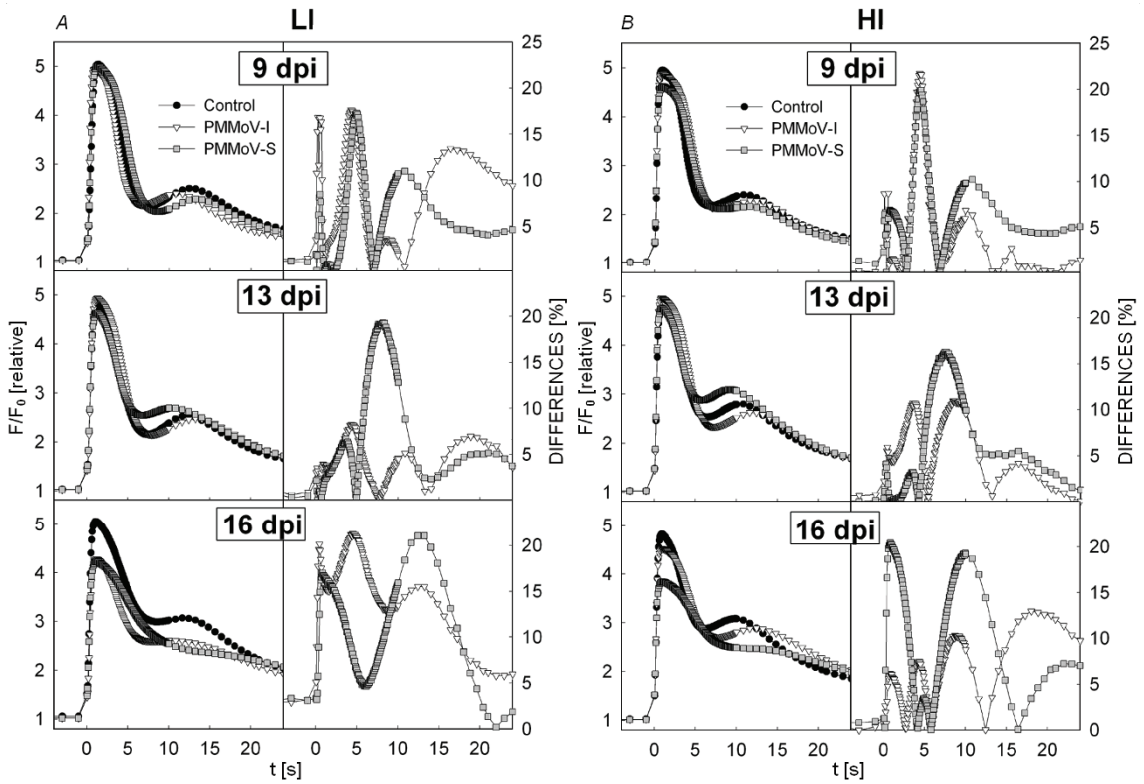

Fig. 6. Chl-F induction transients registered under protocol 3 and elicited by low (LI, *A*) and high (HI, *B*) irradiance in AS leaves from control and infected plants (*left panels*). Chl-F transients represent averages of Chl-F signal integrated over the whole AS leaves from control as well as PMMoV-I and PMMoV-S infected plants at different dpi. Differences [%] between control and infected plants at different dpi are displayed in the *right panels*. LI: 50 μmol(photon) m^{-2} s^{-1}; HI: 200 μmol(photon) m^{-2} s^{-1}. Fluorescence values were normalized to F_0. The transients and the transient relative differences are shown for plants at 9, 13, and 16 dpi.

We proved that R can be used not only for the PMMoV-S infection, on which the classifier was trained, but also for the detection of PMMoV-I infection due to the similarity in observed symptoms. We also checked the ability to detect the infection in young symptomatic leaves of both PMMoV-S and PMMoV-I infected plants during the infection (data not shown). In all cases, the PMMoV infection was detected in 100 % of infected plants using combinatorial imaging.

Discussion

Chl-FI has been broadly applied to study biotic stress in plants (Nedbal and Whitmarsh 2004), making it possible to follow the physiological alterations induced in the infected plants (Lichtenthaler and Miehé 1997). Our previous works with PMMoV-infected plants showed that images of both Chl-F (Chaerle *et al.* 2006) and NPQ (Pérez-Bueno *et al.* 2006) reflect the viral distribution on leaves, which, otherwise, remains asymptomatic during the viral infection. In this study, conventional and combinatorial Chl-F imaging of leaf was used to detect the early phases of infection and to differentiate between the infections with two viral strains of PMMoV on *N. benthamiana* plants.

In agreement with Pérez-Bueno *et al.* (2006), we found that PMMoV-I infection induced in the AS leaf from the host plant a complex and characteristic NPQ pattern from 16−17 dpi onwards (Figs. 3*A,B* and 4). This pattern is better defined in PMMoV-S infected plants, correlating with the higher virulence of this viral strain. NPQ pattern at 17 dpi corresponds to the viral location in these leaves at the same infection points, tested by tissue print (Chaerle *et al.* 2006, Pérez-Bueno *et al.* 2006). Changes on the NPQ pattern reflect a functional response to the infection rather than a viral-induced decrease of the leaf Chl content, as we previously demonstrated (Rahoutei *et al*. 2000, Chaerle *et al.* 2006).

Dynamics of NPQ in the leaf regions colonized by the pathogen are a relevant signature of plant pathogenesis (Chou *et al.* 2000, Berger *et al.* 2004) and correlate with the symptom development (Osmond *et al.* 1998, Lohaus *et al.* 2000). The NPQ increase that appears during the acute phase of the infection in tissues surrounding the main veins may be induced by several alternative molecular mechanisms. Viruses disturb the donor site of PS2

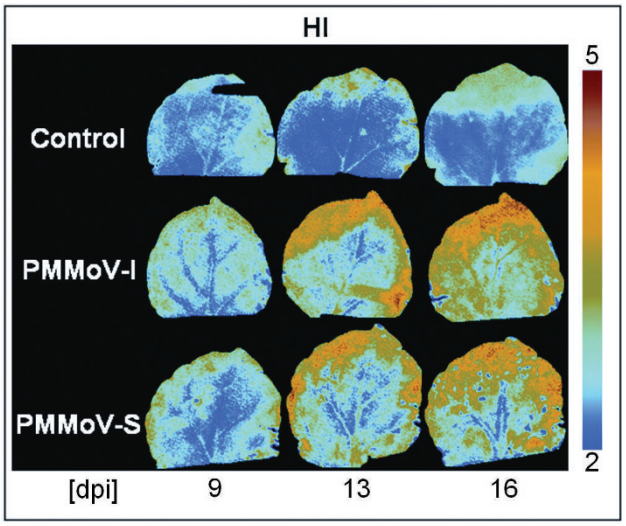

Fig. 7. Images of F_5/F_0 parameter of the representative AS leaves under high irradiance [HI, 200 μmol(photon) m^{-2} s^{-1}] at different dpi captured using measurement protocol 3. F_5 is the chlorophyll fluorescence value at 5 s of the induction curve. Fluorescence values were normalized to F_0.

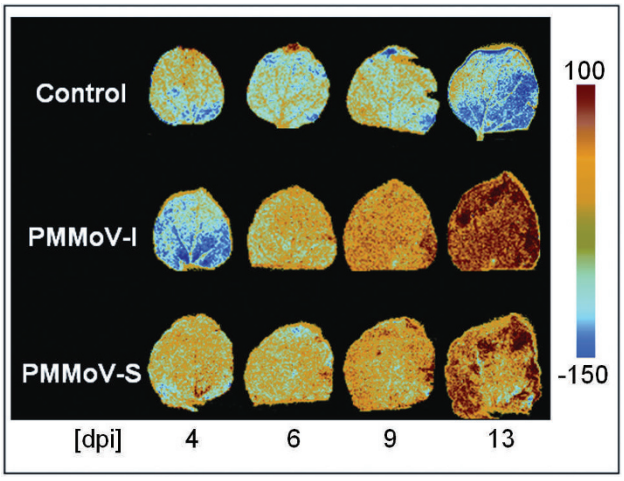

Fig. 8. Combinatorial imaging analysis of the representative AS leaves measured by protocol 2. The resultant image (R; see combinatorial imaging chapters in Materials and methods as well as in Results) obtained by this technique displays the best contrast between control and infected plants. The false colour scale indicates the intensity of the signal in relative units. *Blue area* means pixels classified as "healthy" and red ones correspond to "infected" classified pixels.

due to lower extrinsic protein contents (Rahoutei *et al.* 2000, Pérez-Bueno *et al.* 2004), which may require enhanced protective energy dissipation (van Wijk *et al.* 1993, Critchley and Russell 1994). Viruses also upset the Benson-Calvin cycle (Zhou *et al.* 2004, Sajnani *et al.* 2007) a situation that can increase the trans-thylakoid proton gradient, which modulates the NPQ process (Ruban and Horton 1995). Another process regulating the trans-thylakoid proton gradient is the cyclic electron transport around photosystem 1 (Horton *et al.* 2005), which was proposed to be stimulated during viral infection (Sajnani *et al.* 2007). Independently of its origin, the elevated NPQ during the viral infection could be a host-defence response delaying photoinhibition until the final infection steps (Balachandran *et al.* 1997). Such damage could explain the late decrease of F_V/F_M (point measurements by Rahoutei *et al.* 2000) that was also seen in our experiments at 19−21 dpi (not shown, provided as supplementary data).

Analysis of the Φ_{PS2} kinetic at different infection points revealed that $\Phi_{PS2\text{-}2}$ (at 2 s after switching on the "actinic light") is the only parameter differentiating between the infections with every viral strain in the last infection steps (17−21 dpi). $\Phi_{PS2\text{-}2}$ pattern, like the NPQ_{20} one, also correlates with the viral distribution in the infected leaf (Chaerle *et al.* 2006, Pérez-Bueno *et al.* 2006).

Compared to the detection by NPQ and $\Phi_{PS2\text{-}2}$, the biotic stress was revealed somewhat earlier when the selection of Chl-F parameters was not restricted to the most conventional ones. When we analysed the Chl-F transients under two "actinic" irradiances (Kautsky effect, measuring protocol 3), the first differences between PMMoV-infected and control plants were found at 9 dpi during the initial Chl-F increase and decline from the F_P (Fig. 6), with F_5/F_0 images displaying a heterogeneous Chl-F pattern in infected plants (Fig. 7). Regions emitting less Chl-F corresponded to zones of higher NPQ (Fig. 3*A,B*). In the later post-infection days, there was an increment of kinetic time points displaying differences between infected and control plants (Fig. 6), which could be associated with the senescence process. Changes in the parameter F_5/F_0 may reflect PMMoV-induced alterations on the Benson-Calvin cycle (Zhou *et al.* 2004, Sajnani *et al.* 2007), since this time point is very near to the kinetic peak corresponding to the activation of the cycle (Ireland *et al.* 1984); the fact that the differences between AS leaves from infected plants and control are emphasized by HI is an additional evidence for this contention. Alterations in the slow fluorescence induction transients could be also partly due to inhibition of state transition (Allen and Mullineux 2004).

The detection of the viral infection by the combinatorial imaging (4 dpi, PMMoV-S; 6 dpi, PMMoV-I; Fig. 8; Matouš *et al.* 2006) and by F_5/F_0 imaging (9 dpi) precedes the viral location in AS leaves by tissue printing (Chaerle *et al.* 2006, Pérez-Bueno *et al.* 2006). Conventional Chl-F parameters measured with the protocols 1 and 2 revealed only the PMMoV-infection at an intermediate step (16–17 dpi; Figs. 3 and 4). The fast dynamics of the PMMoV-S infection corresponds to the higher virulence of the strain. The excellent capacity of the combinatorial imaging to reveal very early phases of biotic stress corroborates the earlier studies with bacterial-infected plants (Matouš *et al.* 2006, Berger *et al.* 2007). We found the parameter R robust, since we got successful detection in all evaluated leaves (12 AS

leaves). However, to detect either the PMMoV infection under other environmental conditions or infection by other pathogens, we have to train the system again to obtain new R parameters.

In summary, variations in Chl-F distribution in the *N. benthamiana* AS leaves have the potential to distinguish between PMMoV-I and PMMoV-S infection. Classical Chl-F parameters provided information on the physiological processes, while the analysis of Chl-F transients by combinatorial imaging enabled to detect the infection earlier. Thus, Chl-F imaging is a very useful tool to diagnose and follow the PMMoV infection in *N. benthamiana* plants.

References

Aldea, M., Hamilton, J.G., Resti, J.P., Zangerl, A.R., Berenbaum, M.R., Frank, T.D., de Lucia, E.H.: Comparison of photosynthetic damage from arthropod herbivory and pathogen infection in understory hardwood saplings. – Oecologia **149**: 221-232, 2006.

Allen, J.F., Mullineux, C.W.: Probing the mechanism of state transitions in oxygenic photosynthesis by chlorophyll fluorescence spectroscopy, kinetics and imaging. – In: Papageorgiou, C.G., Govindjee (ed.): Chlorophyll *a* Fluorescence: A Signature of Photosynthesis. Pp. 447-461. Springer, Dordrecht 2004.

Alonso, E., García-Luque, I., Avila-Rincón, M.J., Wicke, B., Serra, M.T., Díaz-Ruiz, J.R.: A tobamovirus causing heavy losses in protected pepper crops in Spain. – J. Phytopathology **125**: 67-76, 1989.

Balachandran, S., Hurry, V.M., Kelley, S.E., Osmond, C.B., Robinson, S.A., Rohozinski, J., Seaton, G.G.R., Sims, D.A.: Concepts of plant biotic stress. Some insights into the stress physiology of virus-infected plants, from the perspective of photosynthesis. – Physiol. Plant. **100**: 203-213, 1997.

Balachandran, S., Osmond, B.C.: Susceptibility of tobacco leaves to photoinhibition following infection with two strains of tobacco mosaic virus under different light and nitrogen nutrition regimes. – Plant Physiol. **104**: 1051-1057, 1994.

Balachandran, S., Osmond, B.C., Daley, F.P.: Diagnosis of the earliest strain-specific interactions between tobacco mosaic virus and chloroplasts of tobacco leaves *in vivo* by means of chlorophyll fluorescence imaging. – Plant Physiol. **104**: 1059-1065, 1994.

Barón, M., Rahoutei, J., Lázaro, J.J., García-Luque, I.: PSII response to biotic and abiotic stress. – In: Mathis, P. (ed.): Photosynthesis: From Light to Biosphere. Vol. 4. Pp. 897-900. Kluwer Academic Publ., Dordrecht – Boston – London 1995.

Berger, S., Benediktyová, Z., Matouš, K., Bonfig, K., Mueller, M.J., Nedbal, L., Roitsch, T.: Visualization of dynamics of plant-pathogen interaction by novel combination of chlorophyll fluorescence imaging and statistical analysis: Differential effects of virulent and avirulent strains of *P. syringae* and of oxylipins on *A. thaliana*. – J. exp. Bot. **58**: 797-806, 2007.

Berger, S., Papadopoulos, M., Schreiber, U., Kaiser, W., Roitsch, T.: Complex regulation of gene expression, photosynthesis and sugar levels by pathogen infection in tomato. – Physiol. Plant. **122**: 419-428, 2004.

Bilger, W., Björkman, O.: Role of the xanthophyll cycle in photoprotection elucidated by measurements of light-induced absorbance changes, fluorescence and photosynthesis in leaves of *Hedera canariensis*. – Photosynth. Res. **25**: 173-185, 1990.

Bonfig, K.B., Schreiber, U., Gabler, A., Roitsch, T., Berger, S.: Infection with virulent and avirulent *P. syringae* strains differentially effects photosynthesis and sink metabolism in *Arabidopsis* leaves. – Planta **225**: 1-12, 2006.

Chaerle, L., Hagenbeek, D., De Bruyne, E., Valcke, R., Van Der Straeten, D.: Thermal and chlorophyll-fluorescence imaging distinguish plant pathogen interaction at an early stage. – Plant Cell Physiol. **45**: 887-896, 2004.

Chaerle, L., Pineda, M., Romero-Aranda, R., Van Der Straeten, D., Barón, M.: Robotized thermal and chlorophyll-fluorescence imaging of *Pepper mild mottle virus* infection in *Nicotiana benthamiana*. – Plant Cell Physiol. **47**: 1323-1336, 2006.

Chou, H.M., Bundock, N., Rolfe, A.S., Scholes, D.J.: Infection of *Arabidopsis thaliana* leaves with *Albugo candida* (white blister rust) causes a reprogramming of host metabolism. – Mol. Plant Pathol. **2**: 99-113, 2000.

Critchley, C., Russell, A.W.: Photoinhibition of photosynthesis *in vivo*: The role of protein turnover in photosystem II. – Physiol. Plant. **92**: 188-196, 1994.

Fukunaga, K.: Introduction to Statistical Pattern Recognition. 2nd Ed. – Academic Press, New York 1990.

García-Luque, I., Ferrero, M.L., Rodríguez, J.M., Alonso, E., de la Cruz, A., Sanz, A.I., Vaquero, C., Serra, M.T., Díaz-Ruíz, J.R.: The nucleotide sequence of the coat protein genes and 3' non-coding regions of two resistance-breaking tobamoviruses in pepper shows that they are different viruses. – Arch. Virol. **131**: 75-88, 1993.

Genty, B., Briantais, J.-M., Baker, N.R.: The relationship between quantum yield of photosynthetic electron transport and quenching of chlorophyll fluorescence. – Biochim. biophys. Acta **990**: 87-92, 1989.

Horton, P., Wentworth, M., Ruban, A.: Control of the light harvesting function of chloroplast membranes: The LHCII-aggregation model for non-photochemical quenching. – FEBS Lett. **579**: 4201-4206, 2005.

Ireland, C.R., Long, S.P., Baker, N.R.: The relationship between carbon dioxide fixation and chlorophyll fluorescence during induction of photosynthesis in maize leaves at different temperatures and carbon dioxide concentrations. – Planta **160**: 550-558, 1984.

Kautsky, H., Hirsch, A.: Neue Versuche zur Kohlensäureassimilation. – Naturwissenschaften **48**: 964-964, 1931.

Kitajima, H., Butler, W.L.: Quenching of chlorophyll fluorescence and primary photochemistry in chloroplasts by dibromothymoquinone. – Biochim. biophys. Acta **376**: 105-115, 1975.

Lamb, E.M., Adkins, S.E., Shuler, K.D., Roberts, P.D.: *Pepper mild mottle virus*. – Gainesville FL: EDIS, HS-808, 2001.

Lichtenthaler, H.K., Babani, F.: Light adaptation and senescence of the photosynthetic apparatus. Changes in pigment composition, chlorophyll fluorescence parameters and photosynthetic activity. – In: Papageorgiou, G.C., Govindjee (ed.): Chlorophyll *a* Fluorescence: A Signature of Photosynthesis.

Pp. 713-736. Springer, Dordrecht 2004.

Lichtenthaler, H.K., Miehé, J.A.: Fluorescence imaging as a diagnostic tool for plant stress. – Trends Plant Sci. **2**: 316-320, 1997.

Lichtenthaler, H.K., Rinderle, U.: The role of chlorophyll fluorescence in the detection of stress conditions in plants. – CRC crit. Rev. anal. Chem. **19**: S29-S85, 1988.

Lohaus, G., Heldt, H.W., Osmond, C.B.: Infection with phloem limited *Abutilon mosaic virus* causes localized carbohydrate accumulation in leaves of *Abutilon striatum*: relationships to symptom development and effects on chlorophyll fluorescence quenching during photosynthetic induction. – Plant Biol. **2**: 161-167, 2000.

Matouš, K., Benediktyová, Z., Berger, S., Roitsch, T., Nedbal, L.: Case study of combinatorial imaging: What protocol and what chlorophyll fluorescence image to use when visualizing infection of *Arabidopsis thaliana* by *Pseudomonas syringae*? – Photosynth. Res. **90**: 243-253, 2006.

Maxwell, K., Johnson, G.N.: Chlorophyll fluorescence – a practical guide. – J. exp. Bot. **51**: 659-668, 2000.

Nedbal, L., Březina, V.: Complex metabolic oscillations in plants forced by harmonic irradiance. – Biophys. J. **83**: 2180-2189, 2002.

Nedbal, L., Březina, V., Adamec, F., Štys, D., Oja, V., Laisk, A., Govindjee: Negative feedback regulation is responsible for the non-linear modulation of photosynthetic activity in plants and cyanobacteria exposed to a dynamic light environment. – Biochim. biophys. Acta **1607**: 5-17, 2003.

Nedbal, L., Soukupová, J., Kaftan, D., Whitmarsh, J., Trtílek, M.: Kinetic imaging of chlorophyll fluorescence using modulated light. – Photosynth. Res. **66**: 3-12, 2000.

Nedbal, L., Whitmarsh, J.: Chlorophyll fluorescence imaging of leaves and fruits. – In: Papageorgiou, C.G., Govindjee (ed.): Chlorophyll *a* Fluorescence: A Signature of Photosynthesis. Pp. 389-407. Springer, Dordrecht 2004.

Osmond, C.B., Daley, P.F., Badger, M.R., Lüttge, U.: Chlorophyll fluorescence quenching during photosynthetic induction in leaves of *Abutilon striatum* Dicks infected with Abutilon mosaic virus observed with a field-portable imaging system. – Bot. Acta **111**: 390-397, 1998.

Pérez-Bueno, M.L., Ciscato, M., vandeVen, M., García-Luque, I., Valcke, R., Barón, M.: Imaging viral infection: studies on *Nicotiana benthamiana* plants infected with the pepper mild mottle tobamovirus. – Photosynth. Res. **90**: 111-123, 2006.

Pérez-Bueno, M.L., Rahoutei, J., Sajnani, C., García-Luque, I., Barón, M.: Proteomic analysis of the oxygen-evolving complex of photosystem II under biotic stress. Studies on *Nicotiana benthamiana* infected with tobamoviruses. – Proteomics **4**: 418-425, 2004.

Pudil, P., Novovicova, J., Kittler, J.: Floating search methods in feature selection. – Pattern Recognition Lett. **15**: 1119-1125, 1994.

Rahoutei, J., Barón, M., García-Luque, I., Droppa, M., Neményi, A., Horvath, G.: Effect of tobamovirus infection on the thermoluminiscence characteristics of chloroplast from infected plants. – Z. Naturforsch. **54c**: 634-639, 1999.

Rahoutei, J., García-Luque, I., Barón, M.: Inhibition of photosynthesis by viral infection: Effect on PSII structure and function. – Physiol. Plant. **110**: 286-292, 2000.

Rahoutei, J., García-Luque, I., Cremona, V., Barón, M.: Effect of tobamovirus infection on PSII complex of infected plants. – In: Garab, G. (ed.): Photosynthesis: From Light to Biosphere. Vol. IV. Pp. 2761-2764. Kluwer Academic Publ., Dordrecht – Boston – London 1998.

Roháček, K., Barták, M.: Technique of the modulated chlorophyll fluorescence: basic concepts, useful parameters, and some applications. – Photosynthetica **37**: 339-363, 1999.

Ruban, A.V., Horton, P.: Regulation of non-photochemical quenching of chlorophyll fluorescence in plants. – Aust. J. Plant Physiol. **22**: 221-230, 1995.

Sajnani, C., Zurita, J.L., Doncel, M., Ortega, J.M., Barón, M., Ducruet, J.-M.: Changes in photosynthetic metabolism induced by tobamovirus infection in *Nicotiana benthamiana* studied in vivo by chlorophyll thermoluminescence. – New Phytol. **175**: 120-130, 2007.

Scholes, J.D., Rolfe, S.A.: Photosynthesis in localised regions of oat leaves infected with crown rust (*Puccinia coronata*): quantitative imaging of chlorophyll fluorescence. – Planta **199**: 573-582, 1996.

Schreiber, U., Schliwa, U., Bilger, W.: Continuous recording of photochemical and non-photochemical chlorophyll fluorescence quenching with a new type of modulation fluorometer. – Photosynth. Res. **10**: 51-62, 1986.

Soukupová, J., Smatanová, S., Nedbal, L., Jegorov, A.: Plant response to destruxins visualized by imaging of chlorophyll fluorescence. – Physiol. Plant. **118**: 399-405, 2003.

Swarbrick, P.J., Schulze-Lefert, P., Scholes, J.D.: Metabolic consequences of susceptibility and resistance (race-specific and broad-spectrum) in barley leaves challenged with powdery mildew. – Plant Cell Environ. **29**: 1061-1076, 2006.

Tang, J.Y., Zielinski, R.E., Zangerl, A.R., Crofts, A.R., Berenbaum, M.R., de Lucia, E.H.: The differential effects of herbivory by first and fourth instars of *Trichoplusia ni* (Lepidoptera: Noctuidae) on photosynthesis in *Arabidopsis thaliana*. – J. exp. Bot. **57**: 527-536, 2006.

van Wijk, K.J., Schnettger, B., Graf, H., Krause, G.H.: Photoinhibition and recovery in relation to heterogeneity of photosystem II. – Biochim. biophys. Acta **1142**: 59-68, 1993.

Wetter, C., Conti, M., Alschuh, D., Tabillion, R., van Regemortel, M.H.V.: *Pepper mild mottle virus*, a tobamovirus infecting pepper cultivars in Sicily. – Phytopathology **74**: 405-410, 1984.

Zangerl, A.R, Hamilton, J.G., Miller, T.J., Crofts, A.R., Oxborough, K., Berenbaum, M.R., de Lucia, E.H.: Impact of folivory on photosynthesis is greater than the sum of its holes. – Proc. nat. Acad. Sci. USA **22**: 1088-1091, 2002.

Zhou, Y.H., Peng, Y.H., Lei, J.L., Zou, L.Y., Zheng, J.H., Yu, J.Q.: Effects of potato virus Y^{NTN} infection on gas exchange and photosystem 2 function in leaves of *Solanum tuberosum* L. – Photosynthetica **42**: 417-423, 2004.